

Exploiting Convexity of Neural Networks in Dynamic Operating Envelope Optimization for Distributed Energy Resources

Hongyi Li, *Member, IEEE*, Liming Liu, *Graduate Student Member, IEEE*, Yunyi Li, Zhaoyu Wang, *Senior Member, IEEE*,

Abstract—The increasing penetration of distributed energy resources (DERs) brings opportunities and challenges to the operation of distribution systems. To ensure network integrity, dynamic operating envelopes (DOEs) are issued by utilities to DERs as their time-varying export/import power limits. Due to the non-convex nature of power flow equations, the optimization of DOEs faces a dilemma of solution accuracy and computation efficiency. To bridge this gap, in this paper, we facilitate DOE optimization by exploiting the convexity of input convex neural networks (ICNNs). A DOE optimization model is first presented, comprehensively considering multiple operational constraints. We propose a constraint embedding method that allows us to replace the non-convex power flow constraints with trained ICNN models and convexify the problem. To further speed up DOE optimization, we propose a linear relaxation of the ICNN-based DOE optimization problem, for which the tightness is theoretically proven. The effectiveness of the proposed method is validated with numerical case studies. Results show that the proposed ICNN-based method outperforms other benchmark methods in optimizing DOEs in terms of both solution quality and solution time.

Index Terms—Distributed energy resources, input convex neural network, power distribution system, optimization.

I. INTRODUCTION

THE penetration level of distributed energy resources (DERs), such as solar panels, battery energy storage systems, and responsive loads, is continuously growing in distribution systems [1]. As cost-efficient and low-carbon energy resources, DERs can significantly reduce the operation costs and carbon emissions of the distribution system. According to FERC Order 2222, DERs are encouraged to actively participate in electricity markets alongside traditional generation resources, which further broadens the benefits brought by DERs [2]. However, besides opportunities, DERs also pose significant challenges to the operation of distribution systems.

Although the impact of a single DER is limited, aggregated DERs can have a nontrivial influence on the voltage profile and power flows of the distribution system [3]. Uncoordinated DER aggregations could lead to multiple operational issues, including over-/under-voltages, overloading of lines and transformers, and reverse power flow, which will consequentially result in accelerated insulation degradation and protection

device malfunctions [4]. Thus, it is necessary for system operators and utilities to coordinate the behaviors of aggregated DERs [5]. The coordination of DERs has been a vibrant research area for many years. Both centralized and decentralized optimization methods are proposed by researchers. In Ref. [6], operation models of various DERs are presented. Then, the power schedules of DERs are optimized in a centralized way to unleash the flexibility of DERs. Centralized coordination methods assume that utilities can intervene in the dispatch decisions of DERs [7]. However, for those DERs owned by aggregators, utilities usually cannot directly control their behavior, necessitating distributed coordination methods [8]. In Ref. [9], the authors propose a fully distributed coordination method, which preserves the autonomy of individual DERs while guiding their behaviors. However, tackling power flow constraints with distributed algorithms is intricate, as third-party DERs cannot access the necessary network model [10].

To ensure network integrity without directly controlling DER power, the concept of dynamic operating envelopes (DOEs) is widely adopted by utilities [11]. DOEs are time-varying export/import power limits issued by utilities to individual DERs, based on the available capacity of the distribution systems [12]. Following the assigned DOEs, DERs can participate in local energy markets [13], peer-to-peer trading [14], and demand response programs [15], without threatening the operational constraints of distribution systems. Characterizing DOEs is challenging due to the non-linearity and non-convexity of power flow equations. An existing approach is to adjust and examine DOEs through a series of power flow calculations until all constraint violations are eliminated [16]. Although this approach is easy to implement, it cannot guarantee optimality. Optimization-based approaches are explored in the literature. In Ref. [17]–[20], researchers optimize DOEs with linearized power flow models, which are easy to solve. However, linearized models usually suffer from inaccuracy. To reduce power flow errors, the authors of Ref. [21], [22] iteratively optimize DOEs with a convex inner approximation of power flow equations. In Ref. [22], DOEs are calculated using a three-phase power flow model, accounting for the imbalanced nature of distribution systems. However, when DOEs need to be updated frequently, model-based methods always require a trade-off between accuracy and computation efficiency [23].

To ease computation burdens, various data-driven power flow models are studied by researchers. In Ref. [24], [25], re-

H. Li, L. Liu, Y. Li, and Z. Wang are with the Department of Electrical and Computer Engineering, Iowa State University, Ames, IA 50011 USA (email: hongyili@iastate.edu; limingl@iastate.edu; liyunyi@iastate.edu; wzy@iastate.edu). (Corresponding author: Zhaoyu Wang.)

gression models are proposed to approximate the relationship between bus power, voltage, and power flows, based on smart meter data. Similar ideas are applied in Ref. [26] for DOE calculation. In Ref. [27], the authors point out that multilayer perceptrons (MLPs) can learn and replicate intractable power flow constraints with mixed-integer linear counterparts, which can be optimized by commercial solvers. However, many integer variables will be introduced to approximate the power flow of large-scale distribution systems, leading to a significant increase in computation burden [28]. Different from MLPs, input convex neural networks (ICNNs) can be reformulated into a group of non-linear convex functions [29], making it appealing for downstream optimization tasks, such as optimal power flow [30], [31]. In Ref. [32], the authors relax the ICNN model into a group of linear constraints, further simplifying the optimization. However, as a promising candidate, how to exploit the convexity of ICNN in DOE optimization still awaits investigation.

In this paper, we propose an ICNN-based method to characterize DOEs for DERs in the distribution system. The optimization model for DOE is first established with various operational constraints. By reformulating the optimization problem, we propose an ICNN-based method to replicate the non-convex power flow constraints with linear counterparts, which is easy for commercial solvers to optimize. The equivalence between the reformulated form and the original ICNN is theoretically proved. To efficiently train ICNNs and solve the reformulated problem, we propose a constraint retrenchment strategy based on the structure of the distribution network. Experiment results show that the proposed ICNN-based method achieves satisfactory performance in both accuracy and computation efficiency. The main contributions of this paper are threefold:

- 1) We develop a comprehensive DOE optimization model for DERs in the distribution system, considering voltage limits, thermal capacities, and reverse power flow limits. After reformulating the DOE optimization problem, the operational constraints are handled by individual ICNN models in a modularized way.
- 2) We propose a constraint embedding method to encode operational constraints as a violation-regularization layer of the trained ICNN. In this way, ICNNs can learn the physical quantities of distribution systems, thereby improving the adaptivity of constraint parameter changes.
- 3) With the constraint embedding method, the ICNNs are translated into linear inequality constraints, replacing the intractable non-convex power flow in the DOE optimization problem. The proposed ICNN-based DOE optimization method significantly reduces computation complexity without compromising accuracy.
- 4) To reduce computation burdens in the training phase and improve optimization efficiency, we propose a constraint retrenchment strategy to prune out unbinding constraints of the DOE optimization problem based on the distribution system structure.

The remainders of this paper are organized as follows: In Section II, the DOE optimization problem is formulated. The

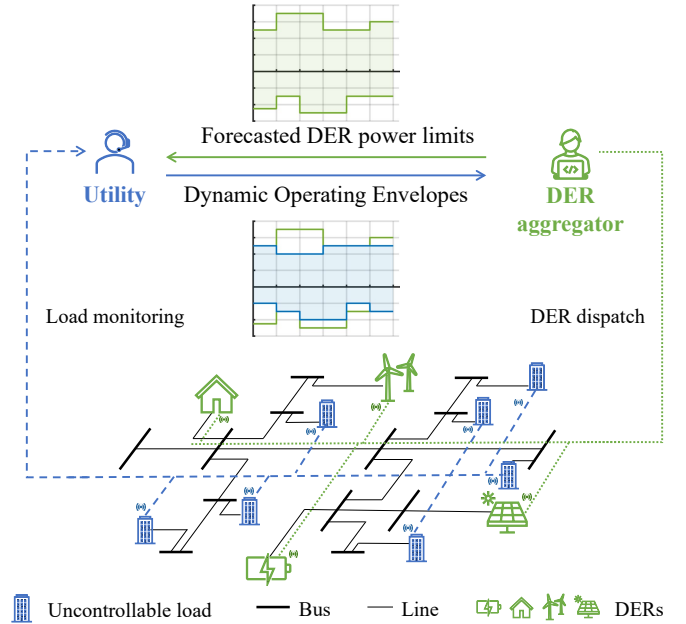


Fig. 1. DOE optimization framework for DERs in the distribution system.

proposed ICNN-based method is presented in Section III. In Section IV, the effectiveness of the proposed DOE optimization method is demonstrated through numerical case studies. Finally, Section V concludes the paper.

II. DYNAMIC OPERATING ENVELOPES FOR DISTRIBUTED ENERGY RESOURCES

In this section, we first introduce the framework for calculating DOEs in distribution systems. Then, we present the DOE optimization problem for DERs and reformulate the problem for ICNN-based solving.

A. Dynamic Operating Envelope Calculation Framework

In the distribution system, there are uncontrollable loads and DERs. We assume that with load monitoring devices, utilities can accurately estimate the power consumption trends of uncontrollable loads. DERs are managed by DER aggregators, which are responsible for forecasting the available power of DERs. The calculation of DOEs for DERs involves two-way communications. As shown in Fig. 1, with the forecasts, DER aggregators send prospective upper and lower DER power limits to the utility. The utility examines the upper and lower limits based on anticipated load levels and determines DOEs for each DER. Here, the utility only reduces the upper limit or increases the lower limit to ensure that no operational constraint is breached. Then, DOEs are issued to DER aggregators and used to constrain the power of individual DERs.

B. DOE Optimization Problem

Before presenting the DOE optimization problem, we outline some necessary notations first. In this paper, we consider a radial distribution network and use j and \mathcal{M} to denote the

index and the set of buses. The direct downstream buses of bus j are included in set \mathcal{N}_j^- . The line set is denoted by \mathcal{E} , where $(i, j) \in \mathcal{E}$ means there is a line connecting bus i and j . For line (i, j) , we use r_{ij} , x_{ij} , P_{ij} , Q_{ij} and $|I_{ij}|$ to denote its resistance, reactance, active and reactive power flow, and current magnitude. With a slight abuse of symbols, we also use j to index the DER connected to bus j . Symbols t and \mathcal{T} denote the index and the set of time intervals in the DOE optimization problem. As discussed in the previous subsection, for each time interval t , we assume that the DER aggregator forecasts the upper and lower active power limits of DER j , denoted by $p_{j,t}^{\max}$ and $p_{j,t}^{\min}$. For buses without DER, we set $p_{j,t}^{\max} = p_{j,t}^{\min} = 0$. The reactive power of each DER $q_{j,t}^{\text{DER}}$ is assumed to be constant. Both active and reactive power of DERs are modeled as power injections. The active and reactive power of uncontrollable loads monitored by the utility are $p_{j,t}^0$ and $q_{j,t}^0$, respectively. To make the discussions in Section III clear and easy to understand, we define vectors \mathbf{V}_t , \mathbf{I}_t and \mathbf{P}_t . Vector \mathbf{V}_t concatenates the voltage magnitudes $|V_{j,t}|$ of all bus at time t , while vectors \mathbf{I}_t and \mathbf{P}_t consist of current magnitudes $|I_{ij,t}|$ and active powers $P_{ij,t}$ of each line (i, j) in the distribution system.

Based on DERs' power limit forecasts and the load level, the utility solves an optimization problem to determine DOEs for DERs. Taking the upper limit $p_{j,t}^+$ as an example, the DOE optimization problem is formulated as follows:

$$\min_{p_{j,t}^+} w^{\text{DOE}} \sum_{t \in \mathcal{T}} \sum_{j \in \mathcal{M}} |p_{j,t}^{\max} - p_{j,t}^+| + \sum_{t \in \mathcal{T}} w^{\text{loss}} P_t^{\text{loss}} \quad (1a)$$

$$\text{s.t. } p_{j,t}^{\min} \leq p_{j,t}^+ \leq p_{j,t}^{\max}, \quad (1b)$$

$$p_{j,t} = p_{j,t}^0 - p_{j,t}^+, q_{j,t} = q_{j,t}^0 - q_{j,t}^{\text{DER}}, \quad (1c)$$

$$P_{ij,t} = \sum_{k \in \mathcal{N}_j^-} P_{jk,t} + p_{j,t} + r_{ij} |I_{ij,t}|^2, \quad (1d)$$

$$Q_{ij,t} = \sum_{k \in \mathcal{N}_j^-} Q_{jk,t} + q_{j,t} + x_{ij} |I_{ij,t}|^2, \quad (1e)$$

$$|V_{j,t}|^2 = |V_{i,t}|^2 - 2r_{ij}P_{ij,t} - 2x_{ij}Q_{ij,t} + (r_{ij}^2 + x_{ij}^2) |I_{ij,t}|^2, \quad (1f)$$

$$|I_{ij,t}|^2 = \frac{P_{ij,t}^2 + Q_{ij,t}^2}{|V_{i,t}|^2}, \quad (1g)$$

$$\mathbf{V}^{\min} \leq \mathbf{V}_t \leq \mathbf{V}^{\max}, \quad (1h)$$

$$\mathbf{I}_t \leq \mathbf{I}^{\max}, \quad (1i)$$

$$\mathbf{P}_t \geq \mathbf{P}^{\min}. \quad (1j)$$

The objective function (1a) includes two terms. The first term minimizes the deviation of DOE from the original upper limits, and the second term aims to reduce the distribution system's active power loss, denoted by P_t^{loss} . Weighting factors w_{DOE} and w_{loss} adjust the emphasize of DOE optimization. Constraint (1b) ensures that DOE lies within the original upper and lower limits. Constraint (1c) defines the net active and reactive loads of bus j . Constraints (1d) - (1g) are the Dist-Flow model describing the power flow equations in a radial distribution system [33]. Note that Constraint (1g) introduces non-convexity to the DOE optimization problem. Constraints (1h) - (1j) are element-wise inequalities. Constraint (1h) avoids

under- and over-voltage issues by limiting bus voltages within lower and upper bounds \mathbf{V}^{\min} and \mathbf{V}^{\max} . Constraint (1i) guarantees that the thermal limits \mathbf{I}^{\max} of the lines are not breached. Defining $P_{ij} > 0$ as the active power flowing from upstream bus i to downstream bus j , constraint (1j) limits the reverse power flow. The reverse power flow limits \mathbf{P}^{\min} are determined by utilities according to their legacy devices, such as overcurrent relays. Since there is no temporal coupling in problem (1), we can optimize the subproblems of each time interval t independently. Thus, in the following discussion, we omit the time index t for simplicity.

In optimization problem (1), we formulate operational constraints (1h) - (1j) as hard constraints. However, in practice, utilities usually allow temporary violation of these constraints, but want to avoid persistent violations. Thus, we reformulate problem (1) by relaxing operational constraints and adding them as penalty terms in the objective function:

$$\min_{p_j^+} w^{\text{DOE}} \sum_{j \in \mathcal{M}} |p_j^{\max} - p_j^+| + w^{\text{loss}} P^{\text{loss}} + w^v \delta^v + w^{\text{ol}} \delta^{\text{ol}} + w^{\text{rpf}} \delta^{\text{rpf}} \quad (2a)$$

$$\text{s.t. } (1b) - (1g), \quad (2b)$$

where δ^v , δ^{ol} and δ^{rpf} are penalty terms for violating constraints (1h), (1i) and (1j). Weighting factors w^v , w^{ol} , and w^{rpf} are used to emphasize different constraints and scale the quantities to comparable levels. The constraint violations are defined as:

$$\delta^v = \mathbf{1}^T [\max(\mathbf{V} - \mathbf{V}^{\max}, 0) + \max(\mathbf{V}^{\min} - \mathbf{V}, 0)], \quad (3)$$

$$\delta^{\text{ol}} = \mathbf{1}^T \max(\mathbf{I} - \mathbf{I}^{\max}, 0), \quad (4)$$

$$\delta^{\text{rpf}} = \mathbf{1}^T \max(\mathbf{P}^{\min} - \mathbf{P}, 0), \quad (5)$$

where the operator $\max(\cdot)$ conducts element-wise comparison.

The reformulated DOE optimization problem (2) allows the operational constraints to be violated in some cases. The weighting factors can be dynamically adjusted according to utilities' risk appetite.

Remark: The optimization of lower bounds p_j^- of DOEs can be achieved by replacing the first term of objective (2a) with $w_{\text{DOE}} \sum_{j \in \mathcal{M}} |p_j^- - p_j^{\min}|$. The DOE optimization methods proposed in Section III are agnostic to the first term of objective (2a) and applicable to both p_j^+ and p_j^- optimizations.

III. INPUT CONVEX NEURAL NETWORK FOR DOE OPTIMIZATION PROBLEM

In this section, we first introduce some preliminaries of ICNN. Then, we propose the constraint embedding method for ICNN and discuss how to translate the trained ICNN models into linear inequality constraints. To further reduce computation burdens, we propose a constraint retrenchment method based on the structure of distribution systems.

A. Preliminaries of Input Convex Neural Networks

1) *Mathematic Model of ICNN:* Proposed in Ref. [29], ICNNs are neural networks that can be interpreted as convex functions of their inputs. As shown in Fig. 2, in addition to the feedforward path, an ICNN has "passthrough" layers from input x to hidden layers, which distinguishes it from other

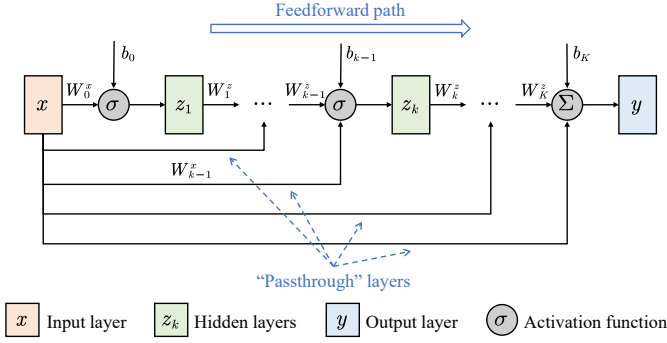


Fig. 2. Illustration of ICNN.

neural networks. For an ICNN with K hidden layers, the mathematical formulation is:

$$z_1 = \sigma(W_0^x x + b_0), \quad (6a)$$

$$z_{k+1} = \sigma(W_k^z z_k + W_k^x x + b_k), \quad k = 1, \dots, K-1, \quad (6b)$$

$$y = W_K^z z_K^l + W_K^x x + b_K, \quad (6c)$$

where x and y are the input and output vectors of ICNN; z_k is the output of hidden layers; W_k^z , W_k^x and b_k are the weights and biases of ICNN; $\sigma(\cdot)$ are the activation functions. Using θ to represent all the weights and biases, the output y can be written as $y = f(x; \theta)$, which is a convex function of x given that the activation functions $\sigma(\cdot)$ are convex and z_k have non-negative weights $W_k^z \geq 0, k = 1, \dots, K-1$. Although non-negativity constraints are added to W_k^z , the value of W_k^x and b_k are not restricted, allowing ICNN to have substantial representation power for complex input-output relationships.

2) *Exact Inference of ICNN*: Inference is the process of obtaining the output of the trained neural network by feeding a new input. Conventionally, neural network inference is completed through algebraic operations. For ICNN, its exact inference can be written as a convex optimization problem. However, a hierarchical combination of convex functions could be very complex. Thus, the optimization-based inference of ICNN is rarely used in practice. One exception is the rectified linear unit (ReLU), which is a piecewise linear activation function:

$$\text{ReLU}(x) = \max(x, 0). \quad (7)$$

Using ReLU as activation functions, the exact inference of ICNN can be written as a linear programming (LP) problem:

$$\min_{z_k, y} y \quad (8a)$$

$$\text{s.t. } z_1 \geq W_0^x x + b_0, \quad (8b)$$

$$z_{k+1} \geq W_k^z z_k + W_k^x x + b_k, \quad k = 1, \dots, K-1, \quad (8c)$$

$$z_k \geq 0, \quad k = 1, \dots, K, \quad (8d)$$

$$y \geq W_K^z z_K^l + W_K^x x + b_K. \quad (8e)$$

Commercial solvers can effectively solve LP problems. In the following subsections, we discuss how to leverage the linearity of ReLU-activated ICNNs for optimizing DOEs for DERs.

B. Learning Power Flow Constraints with ICNN

The key challenge in solving problem (2) is to handle power flow constraints (1d) - (1g) effectively. We assume that utilities have historical operation data, including bus power injections, voltages, line flows, and losses. To facilitate the solving of problem (2), we use ICNNs to learn the mapping from bus power injections to the power loss term and the constraint violation terms. With the proposed methods, we replace the power flow constraints with convex and linear counterparts.

In existing literature, researchers usually let neural networks learn the safe distance to constraint boundaries to guarantee the convexity of the replicated constraints [27], [31]. However, since the calculation of safe distances already involves specific constraint parameters, such as voltage limits, the trained neural networks cannot adapt to parameter changes. To improve the adaptability of the proposed method, we train ICNNs to directly learn the mapping from bus power to active power loss, bus voltages, line current magnitude, and line active power, respectively. To exploit the convexity of ICNN, we adopt ReLU as the activation function throughout the remainder of this paper. Thus, in the following discussions, we directly use the ReLU definition (7) in the mathematical model of ICNN. An ICNN with K hidden layers and ReLU activation functions can be written as:

$$z_1^o = \max(W_0^{x,o} x + b_0^o, 0), \quad (9)$$

$$z_{k+1}^o = \max(W_k^{z,o} z_k^o + W_k^{x,o} x + b_k^o, 0), \quad k = 1, \dots, K-1, \quad (10)$$

$$y^o = W_K^{z,o} z_K^o + W_K^{x,o} x + b_K^o. \quad (11)$$

To simplify notations, we define an index $o \in \{\text{loss, v, ol, rpf}\}$ to distinguish the ICNNs that handle the power loss term, the voltage constraint (3), the overloading constraint (4) and the reverse power flow constraint (5). For the four ICNNs, we define the same input $x = [p_j; q_j]$, which is a column vector concatenating the net active and reactive loads of all buses. The definition of output vector y^o is heterogeneous, which is discussed in detail in the following paragraphs. For simplicity of formulation, we do not specify the number of hidden layers and the number of neurons in each layer of the ICNN, as our proposed methods are agnostic to these configurations.

Since the active power loss P^{loss} is not constrained by upper or lower limits, it is straightforward to set $y^{\text{loss}} = P^{\text{loss}}$. However, for the penalty terms δ^v , δ^{ol} and δ^{rpf} , the corresponding ICNN outputs need to be carefully designed. Otherwise, we cannot exploit the convexity of ICNNs in the optimization problem. Here, we take the voltage limit constraint (1h) as an example and discuss the design of y^v . Assume that we train an ICNN that has an output $y^v = \mathbf{V} = f(x|\theta^v)$. According to the discussion in the last subsection, y^v is a convex function of input x . Substituting $\mathbf{V} = f(x|\theta^v)$ into equation (3) yields:

$$\delta_v = \mathbf{1}^T [\max(f(x|\theta^v) - \mathbf{V}^{\text{max}}, 0) + \max(\mathbf{V}^{\text{min}} - f(x|\theta^v), 0)]. \quad (12)$$

It is obvious that the first term is convex on x , as it involves the positive linear combinations of $f(x|\theta^v)$ and a max operator. However, due to the negative sign of $f(x|\theta^v)$, the second term

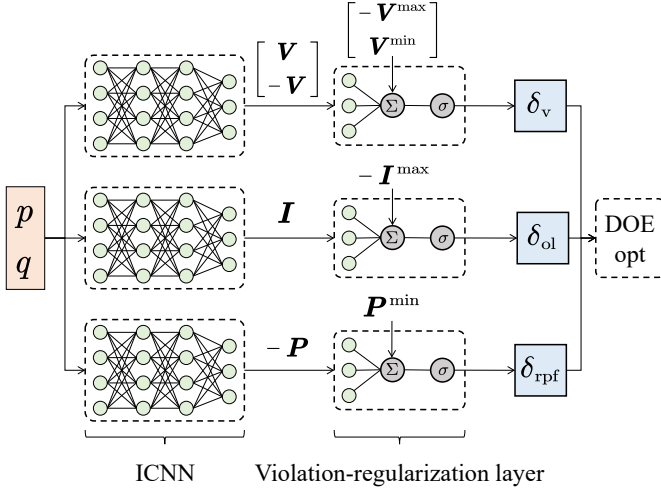


Fig. 3. Proposed constraint embedding method that encodes constraint parameters in violation-regularization layers.

becomes a non-convex function on x . Thus, if the ICNN only learns the physical quantities \mathbf{V} , \mathbf{I} and \mathbf{P} , we can only handle upper limits in constraints (1h) - (1j). For the lower limits, we cannot reformulate the ICNNs into convex counterparts of the power flow equations. To address this issue, we treat upper and lower limits heterogeneously and use separate ICNN outputs to calculate penalty terms. We define the following ICNN outputs:

$$y^v = \begin{bmatrix} \mathbf{V} \\ -\mathbf{V} \end{bmatrix}, y^{ol} = \mathbf{I}, y^{rpf} = -\mathbf{P}, \quad (13)$$

and the corresponding vectors of constraint parameters:

$$\varepsilon^v = \begin{bmatrix} -\mathbf{V}^{\max} \\ \mathbf{V}^{\min} \end{bmatrix}, \varepsilon^{ol} = -\mathbf{I}^{\max}, \varepsilon^{rpf} = \mathbf{P}^{\min}. \quad (14)$$

We take the voltage constraint (1h) as an example again to explain the rationales behind definitions (13) and (14). Substituting $y^v = f(x|\theta^v)$ into equation (3) yields:

$$\delta_v = \mathbf{1}^T \max \{y^v + \varepsilon^v, 0\}, \quad (15)$$

implying that penalty term (3) is convex on the ICNN input x . Similarly, if we substitute y^{ol} and y^{rpf} into equations (4) and (5), δ^{ol} and δ^{rpf} are converted into convex functions of x .

The proposed constraint embedding method is illustrated in Fig. 3. By defining (13) and (14), we encode the parameters of constraints (1h) - (1j) in the violation-regularization layers, which converts the output of ICNNs to the penalty terms defined in equations (3) - (5). The ICNN models with violation-regularization layers can be written as:

$$y^o = f(x|\theta^o), \quad (16)$$

$$\delta^o = \mathbf{1}^T \max (y^o + \varepsilon^o, 0), o \in \{v, ol, rpf\}. \quad (17)$$

Directly plug the ICNN model (16) into the DOE optimization problem (2) yields:

$$\min_{p_j^+} w^{\text{DOE}} \sum_{j \in \mathcal{M}} |p_j^{\max} - p_j^+| + w^{\text{loss}} P^{\text{loss}} + w^v \delta^v + w^{ol} \delta^{ol} + w^{\text{rpf}} \delta^{\text{rpf}} \quad (18a)$$

$$\text{s.t.} \quad (1b), (1c),$$

$$x = [p_j; q_j], \quad (18b)$$

$$y^o = f(x|\theta^o), o \in \{\text{loss}, v, ol, \text{rpf}\}, \quad (18c)$$

$$P^{\text{loss}} = y^{\text{loss}}, \quad (18d)$$

$$\delta^o = \mathbf{1}^T \max (y^o + \varepsilon^o, 0), \forall o \in \{v, ol, \text{rpf}\}. \quad (18e)$$

Off-the-shelf solvers will interpret the optimization model (18) as a mixed-integer linear programming problem (MILP) and solve it with well-developed algorithms such as branch-and-bound. Compared to the original form of problem (2), which involves non-convex power flow constraints, an MILP problem is usually easier to solve. However, due to the integer variables, the solving could still be time-consuming. To further speed up the solving of problem (2), we leverage the exact inference feature of ICNN to relax the problem into a linear form and prove that the relaxation is tight. To this end, we pose non-negativity constraints on the weights of all z_k^o :

$$W_k^{z,o} \geq 0, k = 1, \dots, K. \quad (19)$$

With non-negativity constraint (19), we prove that optimizing the DOE optimization problem (18) is equivalent to optimizing its linear relaxation.

Theorem 1. *Given definitions (13), (14), constraint (19) and the proposed constraint embedding method, optimizing the ICNN-based DOE optimization problem (18) is equivalent to optimizing the following LP problem:*

$$\min_{p_j^+} w^{\text{DOE}} \sum_{j \in \mathcal{M}} |p_j^{\max} - p_j^+| + w^{\text{loss}} \delta^{\text{loss}} + w^v \delta^v + w^{ol} \delta^{ol} + w^{\text{rpf}} \delta^{\text{rpf}} \quad (20a)$$

$$\text{s.t.} \quad (1b), (1c),$$

$$x = [p_j; q_j], \quad (20b)$$

$$z_1^o \geq W_0^{x,o} x + b_0^o, z_1^o \geq 0, \quad \forall o \in \{\text{loss}, v, ol, \text{rpf}\}, \quad (20c)$$

$$z_{k+1}^o \geq W_k^{z,o} z_k^o + W_k^{x,o} x + b_k^o, z_{k+1}^o \geq 0, \quad k = 1, \dots, K-1, \forall o \in \{\text{loss}, v, ol, \text{rpf}\}, \quad (20d)$$

$$\nu^o \geq W_K^{z,o} z_K^o + W_K^{x,o} x + b_K^o + \varepsilon^o, \nu^o \geq 0, \quad \delta^o \geq \mathbf{1}^T \nu^o, \forall o \in \{\text{loss}, v, ol, \text{rpf}\}, \quad (20e)$$

where δ^{loss} , ν^v , ν^{ol} , ν^{rpf} are auxiliary variables and $\varepsilon^{\text{loss}} = 0$.

Proof. The proof of Theorem 1 is derived from the exact inference of ReLU-activated ICNN. Although there are four ICNNs that handle different terms in the objective function, they work independently. Thus, we first prove the equivalence for one ICNN, and the results can be extended to all four ICNNs. Note that weighing factors w^{loss} , w^v , w^{ol} and w^{rpf} are non-negative. With a non-zero weight w^o , solving problem

(20) essentially minimizes the corresponding term δ^o . Since inequality constraints (20e) are convex, minimizing δ^o implies that these constraints must be tight:

$$\delta^o = \mathbf{1}^T \nu^o, \quad (21)$$

$$\nu^o = W_K^{z,o} z_K^o + W_K^{x,o} x + b_K^o + \varepsilon^o \quad \text{or} \quad \nu^o = 0. \quad (22)$$

When $\nu^o \neq 0$, minimizing ν^o is equivalent to minimizing z_K^o , since constraint (19) enforces the weight matrix $W_K^{z,o}$ to be non-negative. Assuming that we have a given input x , minimizing δ^o requires minimizing $W_K^{z,o}$ subject to constraints (20c) and (20d), which coincide with the exact inference of ICNN described in problem (8). Thus, linear relaxations (20c) and (20d) exactly recover the nonlinearity of ICNN models (18c), without introducing integer variables. The equivalence between problem (18) and problem (20) can be easily extended from one ICNN model to multiple ICNN models and from a given x to all possible x that satisfy constraints (1b) and (1c). This completes the proof of Theorem 1. ■

Theorem 1 indicates that, exploiting the convexity and linearity of ICNNs, we can equivalently solve the non-convex DOE optimization problem (2) by solving an LP problem (20). Although ICNN models introduce auxiliary variables to the optimization problem, the linearity of problem (20) allows it to be solved in a very efficient manner by off-the-shelf solvers. As we discussed in the previous section, utilities need to update DOEs for DERs frequently in response to the latest DER power forecast. The improvement in optimization efficiency will significantly reduce the computation time of optimal DOE, especially in large-scale systems with substantial DERs.

C. Constraint Retrenchment Strategy

In the discussions above, we focus on the properties of optimization problems and ICNN models, and let ICNNs learn all the bus voltage magnitudes, line current magnitudes, and line active powers. Intuitively, we need to increase the depth and width of ICNN models as the scale of the distribution system increases. Increasing the number of neurons enhances ICNNs' capability in learning complex mappings, while it also increases the number of variables in the optimization problem. Although the LP form of the DOE optimization problem can be efficiently solved, we still want to keep the number of neurons to its minimum. To this end, we propose a constraint retrenchment strategy that leverages the radial structure of distribution system topologies and prunes out unbinding constraints. With the unbinding constraint set, we can remove some entries of the output vectors y^o and thereby reduce the dimensions of ICNN output layers.

We use Fig. 4, which illustrates a part of a radial distribution system with five buses, to discuss the principle of constraint retrenchment. We define a subset of buses $\tilde{\mathcal{M}} \subset \mathcal{M}$, which contains the buses that only transit power and have no load or DER connected. The set of other buses is defined as $\bar{\mathcal{M}} = \mathcal{M} - \tilde{\mathcal{M}}$. For the buses in set $\tilde{\mathcal{M}}$, e.g., bus 2 and bus 3 in Fig. 4, their voltage magnitudes are bounded by the voltage magnitudes of the adjacent buses, i.e., bus 1, bus 4, and bus 5. Assume that we set the same upper and lower voltage limits

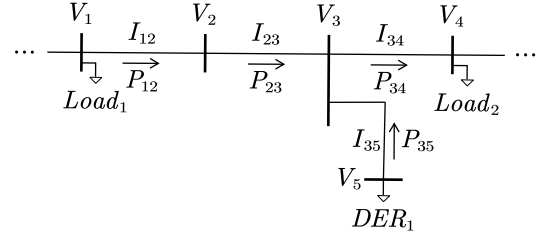


Fig. 4. Illustration of a radial distribution system.

for all buses, if the voltage magnitudes of buses in $\tilde{\mathcal{M}}$ are within the limits in constraint (1h), the voltage limits of buses in $\bar{\mathcal{M}}$ are not breached. Thus, for DOE optimization, we can let ICNN learn the voltage magnitudes of buses in $\tilde{\mathcal{M}}$, instead of all buses in \mathcal{M} . Similarly, if the same thermal capacity is posed to all lines, the current magnitude of line (2,3) is unlikely to reach the limit before violation of the thermal capacities of line (1,2), line (3,4), and line (3,5). Therefore, we can let ICNN focus on the current magnitudes of the lines that are connected to a bus in $\tilde{\mathcal{M}}$, instead of all lines. Finally, since reverse power flow only happens when DERs are injecting power into the grid, we can let ICNN prioritize the active power of the immediate upstream lines of DER buses. After retrenching, ICNNs learn the mapping between fewer variables, reducing the number of neurons in ICNN and the number of variables in the equivalent problem (20). Thus, computation burdens can be reduced.

IV. CASE STUDY

In this section, the effectiveness of the proposed method is validated using a modified IEEE 123-bus test feeder, which is a three-phase unbalanced distribution system. First, we demonstrate the accuracy of ICNN in learning the mapping between physical quantities in the distribution system. Then, the performance of the ICNN-based DOE optimization method is compared with benchmark methods to demonstrate the advantage of the proposed method.

A. Experiment Setup

Test system: The IEEE 123-bus test feeder is a radial distribution system at a nominal voltage of 4.16 kV, featuring unbalanced loading. In the system, there are three-phase, two-phase, and single-phase lines, making the power flow model more complex. To test the DOE optimization problem, we install two DERs in the test system. Table I outlines the locations, upper/lower active power limits, and reactive power setpoints of individual DERs. The system topology and DER locations are visualized in Fig 5. We use OpenDSS [34] to validate the experiment results, whose power flow solutions are considered accurate. We also use the OpenDSS model to generate 30,000 power flow snapshots for ICNNs to learn, by randomly sampling the active and reactive power of the buses. We assume the following limits for the modified IEEE 123-node test feeder: $v^{\min} = 0.9$ p.u., $v^{\max} = 1.1$ p.u., $I^{\max} = 500$ A and $P^{\min} = -125$ kW. The active and reactive load profiles are synthesized based on smart meter data in the

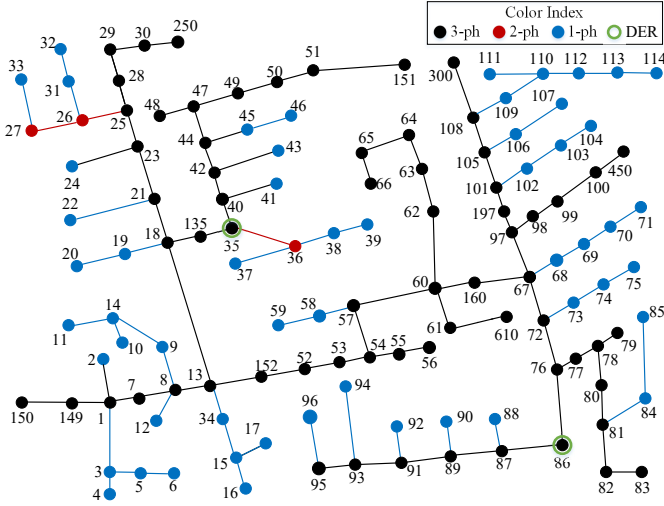


Fig. 5. Modified IEEE 123-bus test feeder system.

TABLE I
DER CONFIGURATIONS.

DER #	Bus	p_j^{\max} (kW)	p_j^{\min} (kW)	q_j (kVar)
1	35	800	0	80
2	86	500	-500	0

Midwest U.S. The power profiles of DERs are synthesized from a solar farm and an electric vehicle charging station in the Midwest U.S.

Benchmarks: To validate the effectiveness of the ICNN-based method, we compare it with two benchmark methods:

- 1) **B0:** DER power takes the upper limit for p_j^+ and lower limit for p_j^- , without considering DOE.
- 2) **B1:** Proposed ICNN-assisted DOE optimization method with linear relaxation, as shown in problem (20).
- 3) **B2:** Proposed ICNN-assisted DOE optimization method without linear relaxation, as shown in problem (18).
- 4) **B3:** Adopt linear DistFlow (LinDistFlow) [35] model to replace power flow constraints and optimize DOE in problem (2). The formulation is provided in Appendix A.
- 5) **B4:** Use ReLU-activated MLPs that share the same hidden layer configurations and input-output with the ICNNs. The DOE optimization problem with MLPs is reformulated into MILP problems, inspired by Ref. [27].

The above benchmark methods are implemented using a PC

TABLE II
HIDDEN LAYER CONFIGURATION AND NMAE OF NEURAL NETWORKS.

Hidden layer configuration	NMAE	
	ICNN	MLP
y^{loss} [128,64]	0.00031	0.00020
y^v [256,256,128,128]	0.00059	0.00055
y^{pl} [256,256,128,64]	0.0026	0.0021
y^{rpf} [128,64]	0.00035	0.00039

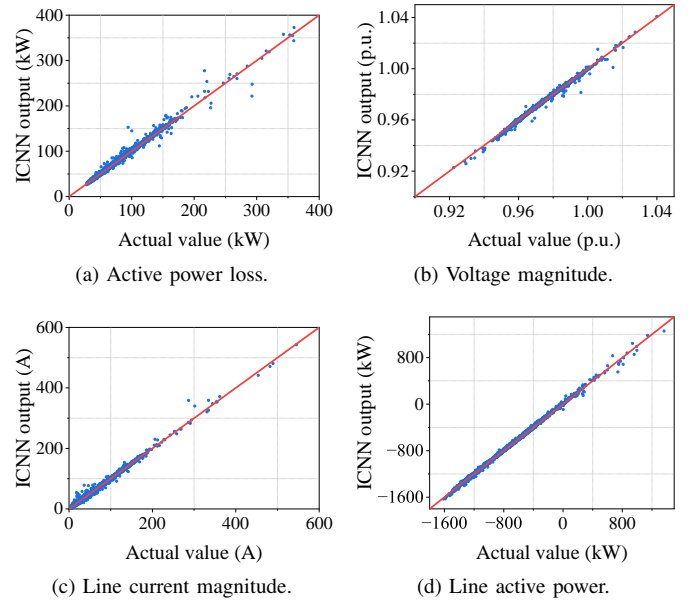


Fig. 6. Comparison of ICNN outputs with actual values.

with an Intel(R) Xeon(R) W-1370 CPU and 32 GB RAM. Gurobi is used as the optimization solver [36].

B. Accuracy of ICNN

To benchmarks B1, B2, and B4, we train ICNNs and MLPs to learn the mapping from bus power to active power loss, bus voltage magnitude, line current magnitude, and line active power. The configurations of neural networks and the normalized mean absolute error (NMAE) are outlined in Table II.

The metric NMAE is defined as the mean absolute error divided by a normalization factor:

$$\text{NMAE}_y = \frac{1}{n} \sum_{i=1}^n \frac{|\hat{y}_i - y_i|}{\tilde{y}}, \quad (23)$$

where n is the sample number of testing data; \hat{y}_i and y_i are the ICNN output value and actual value of the i th sample; \tilde{y} is the normalization factor. In this paper, we use the nominal voltage, substation transformer rated power, and line rated current as the normalization factors for voltage, power, and current, respectively. As shown in Table II, although MLPs' NMAE is slightly lower, ICNNs demonstrate competitive and satisfactory performance in learning the desired mappings.

To further illustrate the accuracy of the ICNNs, we visualize the ICNN outputs versus the actual values in Fig. 6. The blue dots are data points taking the actual values as x-values and the ICNN output as y-values. The red lines are reference lines with slopes equal to one. The blue dots are concentrated around the red lines, implying that for most of the data points in the testing data, the ICNN outputs are very close to the actual values, which further indicates ICNNs' capability in learning and replicating the power flow equations.

C. Effectiveness of ICNN in DOE optimization

The performances of the proposed method and the benchmarks are compared in terms of objective values and solution

TABLE III
RESULTS OF p_j^+ OPTIMIZATION

	\mathcal{J}_1	\mathcal{J}_2	\mathcal{J}_3	\mathcal{J}	Time (s)
B0	0	14.16	927.52	941.68	-
B1	30.87	14.90	0	45.77	0.19
B2	30.87	14.90	0	45.77	12.03
B3	63.80	15.66	0	79.46	1.07
B4	61.42	15.60	0	77.02	900

TABLE IV
RESULTS OF p_j^- OPTIMIZATION

	\mathcal{J}_1	\mathcal{J}_2	\mathcal{J}_3	\mathcal{J}	Time (s)
B0	0	45.28	14633.43	14678.71	-
B1	170.75	35.14	0	205.90	0.20
B2	170.75	35.14	0	205.90	12.10
B3	257.06	30.80	0	287.86	1.05
B4	428.20	27.44	0	455.64	900

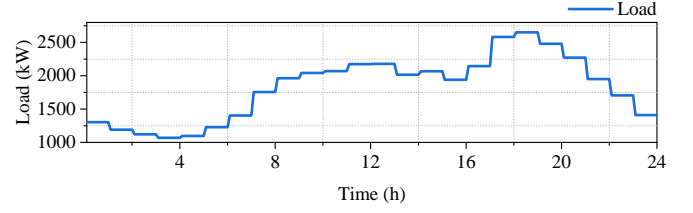
time. To showcase the advantages and disadvantages of each method, we split the objective (2a) into three terms:

$$\mathcal{J} = \underbrace{w^{\text{DOE}} \sum_{j \in \mathcal{M}} |p_j^{\text{max}} - p_j^+|}_{\mathcal{J}_1} + \underbrace{w^{\text{loss}} P^{\text{loss}}}_{\mathcal{J}_2} + \underbrace{w^v \delta^v + w^{\text{ol}} \delta^{\text{ol}} + w^{\text{rpf}} \delta^{\text{rpf}}}_{\mathcal{J}_3}. \quad (24)$$

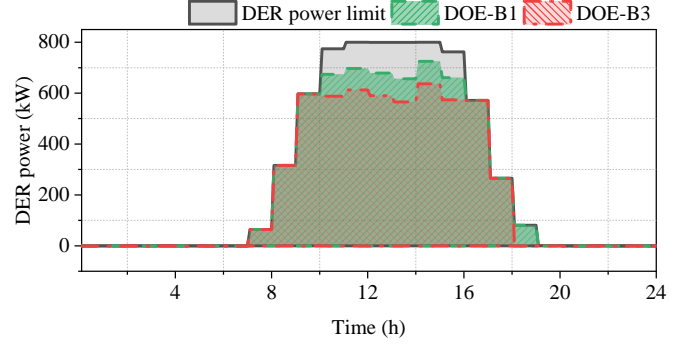
Here, \mathcal{J}_1 denotes the deviation between the optimized DOEs and the original power limits of DERs; \mathcal{J}_2 quantifies the power loss of the system; \mathcal{J}_3 indicates constraint violations of the system. Since DOEs are used to ensure network integrity, we expect \mathcal{J}_3 to be minimized to zero, i.e., constraints (1h) - (1j) are satisfied. In this context, we prefer DOEs that minimize the deviation from original DER power limits and reduce losses, i.e., the smaller \mathcal{J}_1 and \mathcal{J}_2 , the better.

We first analyze the optimization results of one snapshot in detail. The results of optimizing p_j^+ and p_j^- are summarized in Table III and IV, respectively. Benchmark B0 shows the result of unrestrained DER power. If DERs operate at p_j^{max} , the reverse power flow constraint (1j) will be violated, while if DERs operate at p_j^{min} , voltage and overloading constraints will be violated, both resulting in large values of \mathcal{J}_3 . Thus, it is necessary to calculate DOEs to constrain the power of DERs and avoid constraint violation.

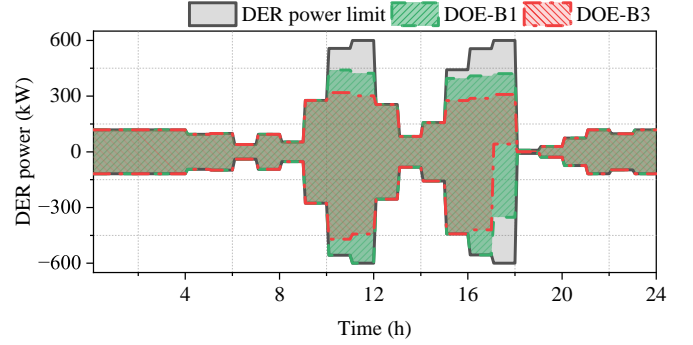
B1 and B2 are ICNN-based methods proposed in this paper, which achieve the lowest objective value \mathcal{J} in both p_j^+ and p_j^- optimizations, outperforming the rest of the benchmark methods. Eliminating all constraint violations, B1 and B2 generate DOEs with the least deviation from p_j^{max} and p_j^{min} and minimal losses. The results demonstrate that the proposed ICNN-based methods can accurately capture the non-convex power flow relationships and effectively simplify the optimization of DOEs for DERs. Note that the solutions obtained by B1 and B2 are the same, implying that the proposed linear relaxation of ICNN is tight, as we theoretically proved in Theorem 1. With linear relaxation, the solution time of DOE optimization problem (2) reduces from more than 10 seconds



(a) Overall active power load of the test system.



(b) DER 1.



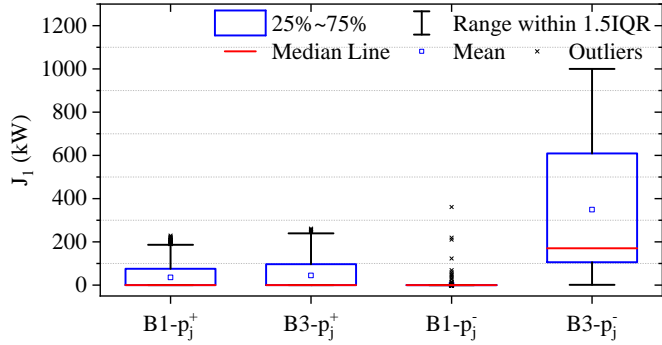
(c) DER 2.

Fig. 7. Illustration of DOEs for DERs in one day.

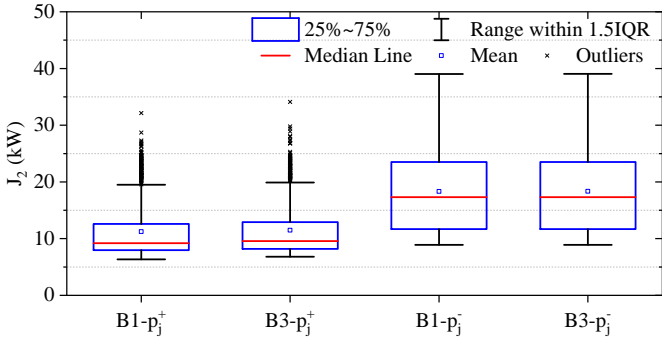
(B2) to less than 0.3 seconds (B1), indicating that the proposed method significantly improves optimization efficiency.

As a model-based linearization method, the solution time of B3 is shorter than B2 but longer than B1. Although performing well in solution time, B3 is more conservative in issuing DOEs. The objective terms \mathcal{J}_1 and \mathcal{J}_2 of B3's results indicate larger deviations of DER power limits and less reduction in power loss. Thus, the DOEs generated by B3 are less optimal than the DOEs generated by B1 and B2. B4 is based on conventional neural networks, which can also accurately learn the power flow relationships, as demonstrated in Table II. However, B4 needs to be reformulated into an MILP problem. In this paper, using the hidden layer configuration specified in Table II results in an MILP with around 2,000 integer variables. In our experiments, Gurobi can only provide a sub-optimal solution of this non-convex MILP problem before it terminates at the 900-second solution time limit. In both cases, our proposed methods B1 and B2 significantly outperform B4 in terms of both solution optimality and solution time.

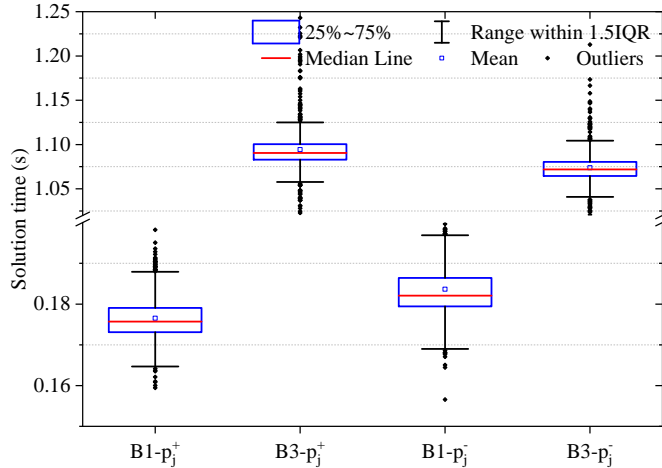
We use hourly time-series data to further examine and compare the benchmarks. Since we have verified the equivalence of our proposed methods B1 and B2, we only show



(a) Objective \mathcal{J}_1 : deviation between optimized DOEs and original power limits.



(b) Objective \mathcal{J}_2 : power loss.



(c) Solution time.

Fig. 8. Comparison of benchmark methods over time-series data.

the results of B1 in the following discussions. B4 is excluded due to its excessively long and impractical solution time. The performance of B1 and B3 is compared in the context of no constraint violation, i.e., $\mathcal{J}_3 = 0$. The overall active power loads of the system and optimal DOEs of individual DERs in one day are visualized in Fig. 7. At night, since the load level and the DER power are both relatively lower, the DOEs issued by both B1 and B3 coincide with the original DER power limits. In the daytime, DOEs restrict both DERs from injecting power to the system at their upper bound to avoid reverse power flow. As shown in Fig. 7b and Fig. 7c, B3 is more conservative than B1 and sets lower upper limits for both DER

1 and DER 2. Since DER 1 is a PV, the lower limit of its DOE remains zero throughout the day. The power demand of DER 2 needs to be restricted by the lower limit of its DOE during peak hours, typically for the purpose of avoiding overloading of lines. We observe that B3 is overly conservative at some time intervals. For example, during hours 10-12, B3 increases the lower power limit of DER 2, which is unnecessary, while B1 is capable of issuing a more reasonable DOE to DER 2 without shifting its lower power limit during these time intervals. Overall, our proposed method B1 generates a wider DOE than B3, allowing DER aggregators to dispatch DERs more flexibly.

Fig. 8 compares the performance of B1 and B3 in optimizing hourly DOEs of 960 successive time intervals. Both benchmark methods generate DOEs without constraint violations. As shown in Fig. 8a, our proposed method B1 is less conservative than B3 in issuing DOEs, for both p_j^+ and p_j^- . B1 significantly outperforms B3 in optimizing p_j^- , because B1 is more accurate in capturing power flow relationships. The performance of B1 and B3 in reducing power loss is similar, as shown in Fig. 8b. Thus, overall, B1 outperforms B3 in minimizing the objective of the DOE optimization problem (2), especially in p_j^- cases. As shown in Fig. 8c, the average solution time of B1 is 83.87% and 82.90% shorter than the solution time of B3. In summary, compared to the LinDistFlow model B3, the proposed ICNN-based method B1 has higher accuracy in modeling power flow relationships and better computation efficiency in optimizing DOEs for DERs, implying a great potential of the proposed method to facilitate DER integration in real-world practices.

V. CONCLUSION

In this paper, we exploit the convexity and linearity of ICNNs for the optimization of DOEs to facilitate DER integration in the distribution system. First, we present the DOE optimization framework and develop a DOE optimization model that comprehensively considers multiple operation constraints. To address the non-convexity brought by power flow constraints, we reformulate the DOE optimization problem and train ICNN models to replicate power flow relationships. With the proposed constraint embedding method, the trained ICNN models are embedded into the reformulated DOE optimization problem and replace the power flow constraints with mixed-integer counterparts. We further propose a linear relaxation of the ICNN-based DOE optimization model and prove the tightness of the relaxation. Through several case studies, we validate the accuracy of the ICNN models in replicating power flow equations and compare the performance of the proposed methods with benchmark methods. The results show that the proposed ICNN-based method excels in both solution accuracy and optimization efficiency.

APPENDIX A

LINDISTFLOW FORMULATION

Assuming that losses are negligible and defining $v_{j,t} = |V_{j,t}|^2$, equations (1d) - (1g) are simplified to:

$$\sum_{k \in \mathcal{N}_j^-} P_{jk,t} = p_{j,t} + P_{i,j,t}, \quad (25a)$$

$$\sum_{k \in \mathcal{N}_j^-} Q_{jk,t} = q_{j,t} + P_{ij,t}, \quad (25b)$$

$$v_{j,t} = v_{i,t} - 2r_{ij}P_{ij,t} - 2x_{ij}Q_{ij,t}. \quad (25c)$$

Albeit linear, model (25) does not explicitly model line current magnitudes and power losses. To cope with the DOE optimization problem (2), we propose the approximation of loss as:

$$P_t^{\text{loss}} = \sum_{(i,j) \in \mathcal{E}} r_{ij}P_{ij,t}^2 + x_{ij}Q_{ij,t}^2. \quad (26)$$

The overloading constraint (1i) is converted to:

$$P_t \leq P^{\text{max}}, \quad (27)$$

where P^{max} is empirically determined from I^{max} .

REFERENCES

- [1] Z. Wang, B. Chen, J. Wang, and C. Chen, "Networked Microgrids for Self-Healing Power Systems," *IEEE Transactions on Smart Grid*, vol. 7, no. 1, pp. 310–319, Jan. 2016, conference Name: IEEE Transactions on Smart Grid.
- [2] FERC, "Order No. 2222: Participation of Distributed Energy Resource Aggregations in Markets Operated by Regional Transmission Organizations and Independent System Operators," Sep. 2020. [Online]. Available: https://www.ferc.gov/sites/default/files/2020-09/E-1_0.pdf
- [3] K. He, H. Jia, Y. Mu, X. Yu, Y. Zhou, J. Wu, and X. Dong, "Leasing business model for trunk mobile charging stations: from the view of operators," *IEEE Transactions on Transportation Electrification*, pp. 1–1, 2025.
- [4] S. Jang, N. Ozay, and J. L. Mathieu, "Probabilistic constraint construction for network-safe load coordination," *IEEE Transactions on Power Systems*, vol. 39, no. 2, pp. 4473–4485, Mar. 2024.
- [5] Z. Wang, B. Chen, J. Wang, M. M. Begovic, and C. Chen, "Coordinated Energy Management of Networked Microgrids in Distribution Systems," *IEEE Transactions on Smart Grid*, vol. 6, no. 1, pp. 45–53, Jan. 2015.
- [6] N. K. Meena, J. Yang, and E. Zacharis, "Optimisation framework for the design and operation of open-market urban and remote community microgrids," *Applied Energy*, vol. 252, no. June, p. 113399, 2019.
- [7] H. Li, H. Hui, and H. Zhang, "Decentralized Energy Management of Microgrid Based on Blockchain-Empowered Consensus Algorithm With Collusion Prevention," *IEEE Transactions on Sustainable Energy*, vol. 14, no. 4, pp. 2260–2273, Oct. 2023.
- [8] Z. Wang, B. Chen, J. Wang, and J. kim, "Decentralized Energy Management System for Networked Microgrids in Grid-Connected and Islanded Modes," *IEEE Transactions on Smart Grid*, vol. 7, no. 2, pp. 1097–1105, Mar. 2016.
- [9] H. Li, H. Hui, and H. Zhang, "Consensus-based energy management of microgrid with random packet drops," *IEEE Transactions On Smart Grid*, vol. 14, no. 5, pp. 3600–3613, Sep. 2023.
- [10] M. Mahmoodi, L. Blackhall, S. M. Noori R. A., A. Attarha, B. Weise, and A. Bhardwaj, "DER capacity assessment of active distribution systems using dynamic operating envelopes," *IEEE Transactions on Smart Grid*, vol. 15, no. 2, pp. 1778–1791, Mar. 2024.
- [11] H. Moring, S. Jang, N. Ozay, and J. L. Mathieu, "Nodal operating envelopes vs. Network-wide constraints: what is better for network-safe coordination of DERs?" *Electric Power Systems Research*, vol. 234, p. 110702, Sep. 2024.
- [12] M. Z. Liu, L. N. Ochoa, S. Riaz, P. Mancarella, T. Ting, J. San, and J. Theunissen, "Grid and market services from the edge: using operating envelopes to unlock network-aware bottom-up flexibility," *IEEE Power and Energy Magazine*, vol. 19, no. 4, pp. 52–62, Jul. 2021.
- [13] M. M. Hoque, M. Khorasany, M. I. Azim, R. Razzaghi, and M. Jalili, "Dynamic operating envelope-based local energy market for prosumers with electric vehicles," *IEEE Transactions on Smart Grid*, vol. 15, no. 2, pp. 1712–1724, Mar. 2024.
- [14] M. I. Azim, G. Lankeshwara, W. Tushar, R. Sharma, M. R. Alam, T. K. Saha, M. Khorasany, and R. Razzaghi, "Dynamic operating envelope-enabled P2P trading to maximize financial returns of prosumers," *IEEE Transactions on Smart Grid*, vol. 15, no. 2, pp. 1978–1990, Mar. 2024.
- [15] G. Lankeshwara, R. Sharma, M. Alam, R. Yan, and T. K. Saha, "Development and validation of a dynamic operating envelopes-enabled demand response scheme in low-voltage distribution networks," *Applied Energy*, vol. 382, p. 125150, Mar. 2025.
- [16] B. Liu and J. H. Braslavsky, "Computation of robust dynamic operating envelopes based on non-convex OPF for unbalanced distribution networks," *CSEE Journal of Power and Energy Systems*, pp. 1–4, 2024.
- [17] M. Z. Liu, L. F. Ochoa, P. K. C. Wong, and J. Theunissen, "Using OPF-Based Operating Envelopes to Facilitate Residential DER Services," *IEEE Transactions on Smart Grid*, vol. 13, no. 6, pp. 4494–4504, Nov. 2022, conference Name: IEEE Transactions on Smart Grid.
- [18] B. Liu, J. H. Braslavsky, and N. Mahdavi, "Linear OPF-based robust dynamic operating envelopes with uncertainties in unbalanced distribution networks," *Journal of Modern Power Systems and Clean Energy*, vol. 12, no. 4, pp. 1320–1326, Jul. 2024.
- [19] Y. Gao, X. Xu, Z. Yan, and M. Shahidehpour, "Equitable active-reactive power envelopes for distributed energy resources in power distribution systems," *IEEE Transactions on Smart Grid*, vol. 16, no. 2, pp. 1480–1494, Mar. 2025.
- [20] Z. Jiang and Y. Guo, "Bargaining-based approach for dynamic operating envelope allocation in distribution networks," *IEEE Transactions on Smart Grid*, pp. 1–1, 2025.
- [21] N. Nazir and M. Almassalkhi, "Grid-aware aggregation and realtime disaggregation of distributed energy resources in radial networks," *IEEE Transactions on Power Systems*, vol. 37, no. 3, pp. 1706–1717, May 2022.
- [22] M. R. Alam, P. T. H. Nguyen, L. Naranpanawe, T. K. Saha, and G. Lankeshwara, "Allocation of dynamic operating envelopes in distribution networks: technical and equitable perspectives," *IEEE Transactions on Sustainable Energy*, vol. 15, no. 1, pp. 173–186, Jan. 2024.
- [23] M. Yang, G. Qiu, J. Liu, Y. Liu, T. Liu, Z. Tang, L. Ding, Y. Shui, and K. Liu, "Topology-Transferable Physics-Guided Graph Neural Network for Real-Time Optimal Power Flow," *IEEE Transactions on Industrial Informatics*, pp. 1–16, 2024.
- [24] Y. Liu, N. Zhang, Y. Wang, J. Yang, and C. Kang, "Data-Driven Power Flow Linearization: A Regression Approach," *IEEE Transactions on Smart Grid*, vol. 10, no. 3, pp. 2569–2580, May 2019, conference Name: IEEE Transactions on Smart Grid.
- [25] Y. Zhang, L. Guo, Y. Liu, Z. Wang, X. Li, L. Bai, and C. Wang, "Nonlinearity-Adaptive Data-Driven Power Flow Constraint for Distribution Network Optimization," *IEEE Transactions on Power Systems*, vol. 39, no. 1, pp. 341–354, Jan. 2024, conference Name: IEEE Transactions on Power Systems.
- [26] A. Kumarawadu, M. I. Azim, M. Khorasany, R. Razzaghi, and R. Heidari, "Smart meter data-driven dynamic operating envelopes for DERs," *Applied Energy*, vol. 384, p. 125469, Apr. 2025.
- [27] G. Chen, H. Zhang, H. Hui, N. Dai, and Y. Song, "Scheduling Thermostatically Controlled Loads to Provide Regulation Capacity Based on a Learning-Based Optimal Power Flow Model," *IEEE Transactions on Sustainable Energy*, vol. 12, no. 4, pp. 2459–2470, Oct. 2021.
- [28] G. Chen, H. Zhang, and Y. Song, "Efficient constraint learning for data-driven active distribution network operation," *IEEE Transactions on Power Systems*, vol. 39, no. 1, pp. 1472–1484, Jan. 2024.
- [29] B. Amos, L. Xu, and J. Z. Kolter, "Input Convex Neural Networks," in *Proceedings of the 34th International Conference on Machine Learning*. PMLR, Jul. 2017, pp. 146–155, ISSN: 2640-3498.
- [30] L. Zhang, Y. Chen, and B. Zhang, "A Convex Neural Network Solver for DCOPF With Generalization Guarantees," *IEEE Transactions on Control of Network Systems*, vol. 9, no. 2, pp. 719–730, Jun. 2022, conference Name: IEEE Transactions on Control of Network Systems.
- [31] R. Cheng, Y. Yang, W. Liu, N. Liu, and Z. Wang, "Input Convex Neural Network-Assisted Optimal Power Flow in Distribution Networks: Modeling, Algorithm Design, and Applications," Jul. 2024, arXiv:2407.20675 [eess].
- [32] T. Wu and J. Wang, "Transient Stability-Constrained Unit Commitment Using Input Convex Neural Network," *IEEE Transactions on Neural Networks and Learning Systems*, vol. 35, no. 11, pp. 16023–16035, Nov. 2024, conference Name: IEEE Transactions on Neural Networks and Learning Systems.
- [33] M. Baran and F. Wu, "Optimal capacitor placement on radial distribution systems," *IEEE Transactions on Power Delivery*, vol. 4, no. 1, pp. 725–734, Jan. 1989.
- [34] R. C. Dugan, "Open distribution simulations system workshop: using open dss for smart distribution simulations," in *EPRI PQ Smart Distribution 2010 Conference and Exhibition*, 2010, pp. 14–17.
- [35] L. Gan and S. H. Low, "Convex relaxations and linear approximation for optimal power flow in multiphase radial networks," in *2014 Power Systems Computation Conference*, Aug. 2014, pp. 1–9.
- [36] L. Gurobi Optimization, "Gurobi Optimizer Reference Manual," 2022.